Hindawi Publishing Corporation
Mathematical Problems in Engineering
Volume 2012, Article ID 941609, 16 pages
doi:10.1155/2012/941609

Research Article

Model of Mass and Heat Transfer during Vacuum Freeze-Drying for Cornea

Zou Huifen,[1] Ye Sheng,[2] Wang Dexi,[3] Li Huixing,[1] Cao Xiaozhen,[1] and Yan Lijun[1]

[1] *School of Municipal and Environment Engineering, Shenyang Jianzhu University, Shenyang 110168, China*
[2] *Management School, Shenyang Jianzhu University, Shenyang 110168, China*
[3] *School of Chemical Engineering Equipment, Shenyang University of Technology, Liaoyang 111003, China*

Correspondence should be addressed to Zou Huifen, jerry_zou@163.com

Received 22 March 2012; Accepted 3 May 2012

Academic Editor: Zhijun Zhang

Cornea is the important apparatus of organism, which has complex cell structure. Heat and mass transfer and thermal parameters during vacuum freeze-drying of keeping corneal activity are studied. The freeze-drying cornea experiments were operated in the homemade vacuum freeze dryer. Pressure of the freeze-drying box was about 50 Pa and temperature was about −10°C by controlled, and operating like this could guarantee survival ratio of the corneal endothelium over the grafting normal. Theory analyzing of corneal freeze-drying, mathematical model of describing heat and mass transfer during vacuum freeze-drying of cornea was established. The analogy computation for the freeze-drying of cornea was made by using finite-element computational software. When pressure of the freeze-drying box was about 50 Pa and temperature was about −10°C, time of double-side drying was 170 min. In this paper, a moving-grid finite-element method was used. The sublimation interface was tracked continuously. The finite-element mesh is moved continuously such that the interface position always coincides with an element node. Computational precision was guaranteed. The computational results were agreed with the experimental results. It proved that the mathematical model was reasonable. The finite-element software is adapted for calculating the heat and mass transfer of corneal freeze-drying.

1. Introduction

The storage of isolated freeze-drying biological tissue is a significant field in the application of vacuum freeze-drying technology and studies for its mass and heat transfer theory under low-temperature, low-pressure conditions which have already become a hot frontal topic in theoretical researches. The vacuum freeze-drying of cornea (freeze-dry) is the freeze-drying for isolated biological tissue which has to remain active afterwards.

The first step during a freeze-drying process is prefreeze, which could affect the activity and the drying rate of cornea. Drying process is to remove the moisture inside cornea, while heat and mass transfer is progressing on a much harder and more complex level. In a drying process of medicine or food, ambient temperature could be increased moderately to provide sufficient heat or heating the material directly in the second step and the resolution process of adsorbed moisture could hence been accelerated which results in a more cost-effective way of freeze-drying. Time and cost is not a critical factor during a freeze-drying process, it is all about to reduce the risk of cornea being spoiled throughout the drill. Therefore, the time should be minimized in freeze-drying of cornea in order to obtain higher survival chance for corneal endothelial cells. But due to the limitation of corneal cell's configuration, underneath the external surface (endothelial cell and epidermal cell), there is an elastic layer that resists the diffusion of the moisture within the matrix (moisture in the matrix count for 90% of the overall water content). If the temperature of sublimation front is too high, as higher level of vapor in sublimation, the internal pressure in the cornea will rise correspondingly, which leads to two circumstances as follow. (1) If the vacuum degree inside the freeze-drying chamber is high and the pressure is low at the meantime, the inner and outer pressure of cornea would achieve a relatively high level that leads to the exposure of moisture inside the cornea through the external surface. Epidermal cell and endothelial cell might drop off, leading to the whole process become meaningless. (2) If the pressure within the drying chamber is at an appropriate rate with the pressure of the cornea, but the temperature of sublimation interface is swelling up which leads to vapor increase and melting of the freeze-layer, resulting in death or injury of cells and loss of the freeze-drying condition. By calculating the theoretical model, seeking for the appropriate temperature and pressure for the will of freeze-drying experiment results could be insured as being optimized and stabilized.

A number of models on freeze-drying have been mentioned in many researches [1–11] aiming to describe the process. The sorption-sublimation model presented by Liapis and Litchfield is the most widely used one and character as the synch of sorption and sublimation of moisture, also, the removal of bounded water is considered in the equation. The result of this modeling agrees with Moffert's research. However, the model is of one dimension, in the process of freeze-drying, the sublimate interface arises with the drying procedure. Liapis and Litchfield employ a one-dimensional moving interface [12], thus the prerequisite of material applied have to be one-dimension with no bent at any angle. Tang et al. [13] have modified this model into two dimensions to describe the freeze-drying of drugs in the penicillin vial, this 2D model could accurately reflect the position and shape of the sublimation interface, ergo; it can simulate the actual progress. Millman et al. have further the model that presented by Tang [14], in which the new model could allow the material form in arbitrary shape. The characteristics of this model is to involve more factors with less limitation, therefore, it has been widely used. But due to the complexity of the model, and the numerous parameters that have to be considered, the application of this model run encounters difficulties.

Models mentioned above were solved by program which developed by themselves, and studied material is at least more than 5 mm, and the cornea is only 0.6 mm thick. The use of the material has certain degree of difficult as the heat and mass transfer have their own characteristics. This article combine the advancement of Millman's model and finite element analysis software, constructing the 2D model of freeze-drying process of cornea that allow the sublimation and desorption happen simultaneously, taking into account of the removal of bounded moisture. Also, 2D approach has been applied to fix the mobile interface. Small-scale changes base on the present software have been done to simulate the heat and mass transfer

of freeze-drying cornea. The calculated results are basically consistent with the experimental data and more details have described as follows.

2. Establishment of Mathematical Model

2.1. Hypothesis

The establishment of mathematical model is refered to the coupled equation of heat and mass transfer which is developed by Millman. In this article, assumptions have been made as follows, relating to the establishment of finite element model.

(1) The 2D dimensional heat and mass transfer is considered.

(2) The interface thickness was thought to be infinitely small (the assumption has been confirmed in many researches [15]).

(3) The mixture of water vapor and permanent gases flow passes the drying layer.

(4) The concentration of vapor and ice phase equilibrium is at the interface.

(5) The semidry layer is a porous region due to the back of sublimation interface, dry-material, and adsorbed-water (solid phase) were inside the region. The gas consists of vapor and permanent gases, which were considered to maintain thermal equilibrium with the solid phase.

(6) Surface and interface temperature stay unchanged.

(7) The frozen zone is assumed to be uniform and has uniform thermal conductivity, density and specific heat, also it contains small amount of dissolved gases.

(8) Changes of the overall size of cornea are out of question.

(9) The total pressure of the drying chamber was controlled by appropriate-size vacuum pump and required devices (most of the permanent gases in the chamber was considered leak in).

2.2. Mass Transfer Equation

Continuity equations of dry-layer can be expressed as follows:

$$\varepsilon \frac{DC_{gw}}{Dt} + \rho_1 \frac{DC_{sw}}{Dt} + \nabla \cdot N_w = 0, \tag{2.1}$$

$$\varepsilon \frac{DC_{g\text{in}}}{Dt} + \nabla \cdot N_{\text{in}} = 0, \tag{2.2}$$

in which

$$\frac{DC_{sw}}{Dt} = k_g(C^*_{sw} - C_{sw}), \tag{2.3}$$

$$N_w = -k_1 \nabla C_{gw} - k_2 C_{gw} \nabla P, \tag{2.4}$$

$$N_{\text{in}} = -k_3 \nabla C_{g\text{in}} - k_4 C_{g\text{in}} \nabla P, \tag{2.5}$$

$$P = P_w + P_{\text{in}}, \tag{2.6}$$

$$C^*_{sw} = f(P_w, T_1), \tag{2.7}$$

C^*_{sw} is the density of water in solid phase when water-gas equilibrium was achieved.

Equations (2.4) and (2.5) are the mass-trans rate formula of binary mixture pass through the dry zone, based on diffusion equation (Evans et al. [16]) and viscous flow formula (D′Arcy). In the formula, the main vapor diffusion is passing through the dry layer, and escaping by way of Knudsen diffusion and the corresponding total pressure gradient; also with no consideration of surface diffusion and thermal diffusion model as such diffusion is not significant [17]. It has been proved that the role of viscous flow is not that important for N_w and N_{in} [18]. Knudsen diffusion is the most important one in the case of low/permanent gas nonexist. However, main diffusion controls the rate when they do exist. Therefore, (2.4) and (2.5) can be simplified as

$$\begin{aligned} N_w &= -k_1 \nabla C_{gw}, \\ N_{\text{in}} &= -k_3 \nabla C_{g\text{in}}. \end{aligned} \tag{2.8}$$

By (2.1) and (2.4), we obtain:

$$\varepsilon \frac{DC_{gw}}{Dt} + \rho_1 \frac{DC_{sw}}{Dt} = \nabla \cdot (k_1 \nabla C_{gw}). \tag{2.9}$$

By (2.2) and (2.5), we obtain

$$\varepsilon \frac{DC_{g\text{in}}}{Dt} = \nabla \cdot (k_3 \nabla C_{g\text{in}}). \tag{2.10}$$

The work in [17] has proved that permanent gas got a very small change rate; (2.9) could hence be solved without (2.10). Therefore, the following manipulating only includes finite element formulation for (2.9).

In the 2D symmetric space, (2.9) can be expressed as

$$\varepsilon \frac{DC_{gw}}{Dt} + \rho_1 \frac{DC_{sw}}{Dt} = k_1 \left[\frac{\partial}{\partial x} \frac{\partial C_{gw}}{\partial x} + \frac{1}{r} \frac{\partial}{\partial y} \left(r \frac{\partial C_{gw}}{\partial y} \right) \right]. \tag{2.11}$$

Under low pressure, the concentration of water vapor and permanent gases can be expressed by using the ideal gas law:

$$M_i P_i = C_{gi} RT. \tag{2.12}$$

So, (2.11) can be described by the following equation:

$$\frac{\varepsilon M_w}{RT_1}\frac{DP_w}{Dt} + \rho_1 \frac{DC_{sw}}{Dt} = \frac{k_1 M_w}{RT_1}\left[\frac{\partial}{\partial x}\frac{\partial P_w}{\partial x} + \frac{1}{r}\frac{\partial}{\partial y}\left(r\frac{\partial P_w}{\partial y}\right)\right], \tag{2.13}$$

and assuming that

$$A_1 = \frac{\varepsilon M_w}{RT_1}, \qquad A_2 = \frac{k_1 M_w}{RT_1}, \qquad F_1 = \frac{\partial P_w}{\partial x}, \qquad F_2 = \frac{\partial P_w}{\partial y}, \tag{2.14}$$

by (2.13) and (2.14), we obtain

$$A_1 \frac{DP_w}{Dt} + \rho_1 \frac{DC_{sw}}{Dt} = A_2\left[\frac{\partial F_1}{\partial x} + \frac{1}{r}\frac{\partial}{\partial y}(rF_2)\right]. \tag{2.15}$$

2.3. Heat Transfer Equation

In a 2D symmetric space, energy equation for dry-layer is

$$\rho_{1e} C_{P1e}\frac{DT_1}{Dt} - k_{1e}\left[\frac{\partial}{\partial x}\frac{\partial T_1}{\partial x} + \frac{1}{r}\frac{\partial}{\partial y}\left(r\frac{\partial T_1}{\partial y}\right)\right] + C_{Pg}\left[\frac{\partial (N_{tx}T_1)}{\partial x} + \frac{1}{r}\frac{\partial (N_{ty}T_1)}{\partial y}\right] - \Delta H_v \rho_1 \frac{\partial C_{sw}}{\partial t} = 0. \tag{2.16}$$

Frozen layer energy equation is

$$\rho_{\mathrm{II}} C_{P\mathrm{II}}\frac{DT_{\mathrm{II}}}{Dt} - k_{\mathrm{II}}\left[\frac{\partial}{\partial x}\frac{\partial T_{\mathrm{II}}}{\partial x} + \frac{1}{r}\frac{\partial}{\partial y}\left(r\frac{\partial T_{\mathrm{II}}}{\partial y}\right)\right] = 0. \tag{2.17}$$

2.4. Concentration Equation

Moisture concentration change in the dry layer versus time can be described as

$$\frac{DC_{sw}}{Dt} = k_g (C^*_{sw} - C_{sw}). \tag{2.18}$$

2.5. Initial and Boundary Condition

When $t = 0$,

$$\begin{aligned} P &= P^0, \\ T_{\mathrm{I}} = T_{\mathrm{II}} &= T^0, \\ C_{sw} &= C_{sw}^0. \end{aligned} \tag{2.19}$$

When $t > 0$,

$$\begin{aligned} P &= \widehat{P}, \\ T &= \widehat{T}. \end{aligned} \tag{2.20}$$

Equation (2.20) specified the boundary value of pressure and temperature. The concentration equation is an issue relating to initial value, with no consideration of any boundary conditions.

3. The Trajectory of the Sublimation Interface

During the process of drying, the sublimation latent heat was released at the sublimation interface, and the sublimation heat was added as boundary condition when solving a series of control equation. It, hence, becomes necessary to track the location of the interface and impose boundary conditions on the interface spot. The movement of the interface is affirmed by exam the equilibrium of heat at the interface. In the case of noninternal heat source, the heat originates from the dried layer equals to the total heat both from the absorption and the heat flowed to the frozen layer. The heat balance equation can be expressed as follows:

$$k_{\mathrm{II}} \frac{\partial T_{\mathrm{II}}}{\partial n} - k_{1e} \frac{\partial T_1}{\partial n} + N_{tn} C_{Pg} T_1 = -v_n \left(\rho_{\mathrm{II}} C_{P\mathrm{II}} T_{\mathrm{II}} - \rho_1 C_{P1} T_1 \right) - \Delta H_s N_{tn}, \tag{3.1}$$

in which

$$v_n = -\frac{N_{wn}}{\rho_{\mathrm{II}} - \rho_1}. \tag{3.2}$$

The velocity of interface v_n perpendicular to the interface itself, and v_n could conclude from (3.2) in order to obtain the new interface location. Numerous numerical calculation techniques were used to solve the problem of moving interface, in the paper, however, the finite-grid-element method has been used [13], where the sublimation interface was tracked consecutively and the interface was assumed to be boundary condition of the move. The finite grid would be redivided when changes occur in the sublimation interface, by doing this, to fix the interface location always at the unit node. In other words, instead of stay in the unit, the interface location would always be on the outline or node of the unit, and so the boundary conditions would be added on the contour line. Therefore, the equation of both

dry and frozen layers can be solved together with the combination of interface boundary conditions.

4. Finite-Element Formulations

Variational equation within the finite equation defines the formulation (2.15) and (2.18) as

$$\int_{\Omega^e}\left[wA_1\left(\frac{\partial P_w}{\partial t}-g_x\frac{\partial P_w}{\partial x}-g_y\frac{\partial P_w}{\partial y}\right)+A_2\frac{\partial w}{\partial x}F_1+A_2\frac{\partial w}{\partial y}F_2+\rho_1\frac{DC_{sw}}{Dt}w\right]r\,dx\,dy - \oint_{\Gamma^e} w\ \left[A_2F_1n_x+A_2F_2n_y\right]dS=0, \tag{4.1}$$

$$\begin{aligned}&\int_{\Omega^e}\left\{w\rho_{1e}\left(\frac{\partial T_1}{\partial t}-g_x\frac{\partial T_1}{\partial x}-g_y\frac{\partial T_1}{\partial y}\right)+k_{1e}\left[\frac{\partial w}{\partial x}\frac{\partial T_1}{\partial x}+\frac{\partial w}{\partial y}\frac{\partial T_1}{\partial y}\right]\right.\\&\qquad\left.-C_{Pg}\left[\frac{\partial w}{\partial x}(N_{tx}T_1)+\frac{\partial w}{\partial y}(N_{ty}T_1)\right]-\Delta H_v\rho_1\frac{DC_{sw}}{Dt}w\right\}r\,dx\,dy\\&\quad-\oint_{\Gamma^e}\left(k_{1e}\frac{\partial T_1}{\partial x}n_x+k_{1e}\frac{\partial T_1}{\partial y}n_y\right)w\,dS\\&\quad+\oint_{\Gamma^e}C_{Pg}\left[w(N_{tx}T_1)n_x+w(N_{ty}T_1)n_y\right]dS=0,\end{aligned} \tag{4.2}$$

$$\begin{aligned}&\int_{\Omega^e}\left[w\rho_{\mathrm{II}}C_{P\mathrm{II}}\left(\frac{\partial T_{\mathrm{II}}}{\partial t}-g_x\frac{\partial T_{\mathrm{II}}}{\partial x}-g_y\frac{\partial T_{\mathrm{II}}}{\partial y}\right)+k_{\mathrm{II}}\left(\frac{\partial w}{\partial x}\frac{\partial T_{\mathrm{II}}}{\partial x}+\frac{\partial w}{\partial y}\frac{\partial T_{\mathrm{II}}}{\partial y}\right)\right]r\,dx\,dy\\&\quad-\oint_{\Gamma_e}\left(k_{\mathrm{II}}\frac{\partial T_{\mathrm{II}}}{\partial x}n_x+k_{\mathrm{II}}\frac{\partial T_{\mathrm{II}}}{\partial y}n_y\right)w\,dS=0,\end{aligned} \tag{4.3}$$

$$\int_{\Omega^e}w\left[\left(\frac{\partial C_{sw}}{\partial t}-g_x\frac{\partial C_{sw}}{\partial x}-g_y\frac{\partial C_{sw}}{\partial y}\right)-k_g(C^*_{sw}-C_{sw})\right]r\,dx\,dy=0, \tag{4.4}$$

in which w represents the finite element weight equation, Γ^e is the sum of the computational domain Ω^e's boundary, while n_x and n_y are the direction cosine of n. Boundary term in (4.1)–(4.3) can be defined as follows:

water vapor flow

$$N_{wn}=N_{wx}n_x+N_{wy}n_y=A_2F_1n_x+A_2F_2n_y, \tag{4.5}$$

heat flow:

$$\begin{aligned}q_n&=q_xn_x+q_yn_y=-k_{1e}\frac{\partial T_1}{\partial x}n_x-k_{1e}\frac{\partial T_1}{\partial y}n_y\quad(\text{dry area})\\&=-k_{\mathrm{II}}\frac{\partial T_{\mathrm{II}}}{\partial x}n_x-k_{\mathrm{II}}\frac{\partial T_{\mathrm{II}}}{\partial y}n_y\quad(\text{frozen region}),\end{aligned} \tag{4.6}$$

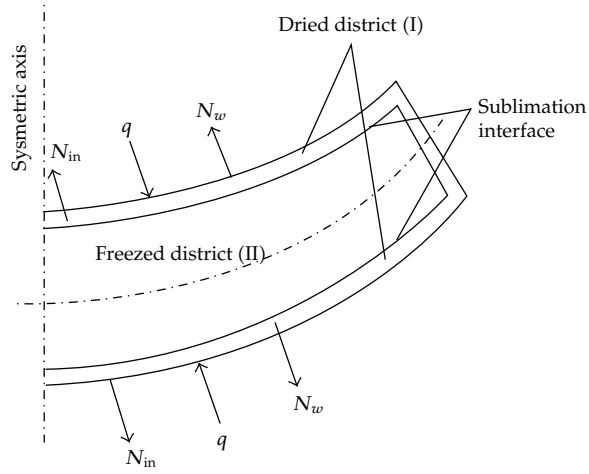

Figure 1: Schematic of cornea freeze drying.

the total flow:

$$N_{tn} = N_{tx}n_x + N_{ty}n_y. \tag{4.7}$$

5. Results and Discussion of the Frozen Model

Figure 1 is an illustration of a sided schematic lyophilized. At the beginning of calculation, the initial dry layer thickness needs to be determined, and the equation would be unsolved when the freeze starts and the thickness of dried layer is zero. Similarly, it is required to determine the residual value of the frozen layer when the frozen layer thickness trends to be zero [19]. As the test results tell, the initial thickness of frozen layer would be 6×10^{-6} m, and for residual layer thickness, the value should be 1×10^{-6} m as shown in Table 1.

5.1. The Relationship between Lyophilized Chamber Pressure and Drying Time

In the process of freeze the cornea, radiation heat is the dominating way of heating. During the radiation heating, sublimation starts at the frozen material surface, which gradually forms an interface between the dried layer and frozen layer (as shown in Figure 1). The heat passes through the porous dried layer by thermal conductivity and spreads to the sublimation interface, adsorbed by the ice sublimation process simultaneously. The vapor emerged from the diffusion spread along the opposite direction of heat from the sublimation interface to the dry layer. Also, the sublimation interface moves inwards gradually until the frozen water disappears and the sublimation come to an end. So, the moving rate of the interface could stand for the lyophilized rate.

The speed of the freeze-dry process depends on the sublimation of ice and the diffusion rate of vapor, the former indicator is also determined by the intensity of heat transfer to the sublimation interface, hence, the drying process is controlled by tow mechanisms. Filled with vapor and small amount of air, the gas thermal conductivity rate inside the dried

Table 1: Parameter values during computing [14, 20, 21].

Nomenclature	Unit	Value
C^*_{sw}	kg water/kg solid	$0.01\exp(2.3(1.36-0.036(T-T^0)))$
C_2	—	0.4428
C_{p1}	kg/kg·K	2.595
$C_{p\mathrm{II}}$	kg/kg·K	1.9678
C_{Pg}	kg/kg·K	1.6747
ρ_1	$\mathrm{kg/m^3}$	209.3
ρ_{II}	$\mathrm{kg/m^3}$	910
ε	—	0.706
ΔH_s	KJ/Kg	2834.6
ΔH_V	KJ/Kg	2499.6
$P_w\vert_{\mathrm{int}\,f}$	Pa	$133.32[\exp(23.9936-2.19\Delta H_s/T_{\mathrm{int}\,f})]$
$D^0_{w,\mathrm{in}}$	$\mathrm{kg\cdot m/s^3}$	$8.729\times10^{-7}(T_0+T_{\mathrm{int}\,f})^{2.334}$
k_{1e}	W/m·K	$0.68(12.98\times10^{-8}P+39.806\times10^{-6})$
k_{II}	W/m·K	0.146
k_g	1/s	1.108×10^{-4}
K_w	$\mathrm{m^2/s}$	$1.429\times10^{-4}(T_0+T_{\mathrm{int}\,f})^{0.5}$

layer arises with the pressure increase. Therefore, when the pressure rises in the freeze-dry chamber, the effective thermal conductivity of the dried layer would arise and provide heat to the sublimation interface which accelerates the process. The driving force of vapor is the differential pressure of the sublimation and dried layer. The vapor pressure on the sublimation interface can be assumed equal to the saturation pressure under the interface temperature. When the temperature of the lyophilized chamber arises, the partial pressure of the dried layer increases which slows down the vapor diffusion rate control by the dried layer differential pressure of mass transfer. Clearly, the pressure of lyophilized chamber impact oppositely to the ice crystal simulation rate and water vapor diffusion rate, that is, to double impact the lyophilize process both boost and retard the process. Apparently, there should be a certain pressure that optimizes the freeze-drying rate [22, 23]. During the cornea lyophilized process, there also exists an optimum value for the chamber, which can both ensure the endothelial cell survival chance and taking into account the lyophilized rate.

Figure 2 shows the lyophilized cornea freeze time under the condition of the pressure 20 Pa, 50 Pa, 80 Pa, 110 Pa. As can be concluded from the figure, the time for freeze dry the cornea basically equals to the pressure when it is below 50 Pa, then as the pressure increases, the time needed increases accordingly. The simulation results and the experimental test afterwards conclude that the chamber pressure should be over 50 Pa if more than 80% of the survival rate is required.

5.2. The Relationship between Temperature of Sublimation Interface and Time of Drying

In the process of freeze-drying, as the ice is sublimating, the interface between the porous dried layer and the frozen layer will be continuously moving backward, inducing the increase

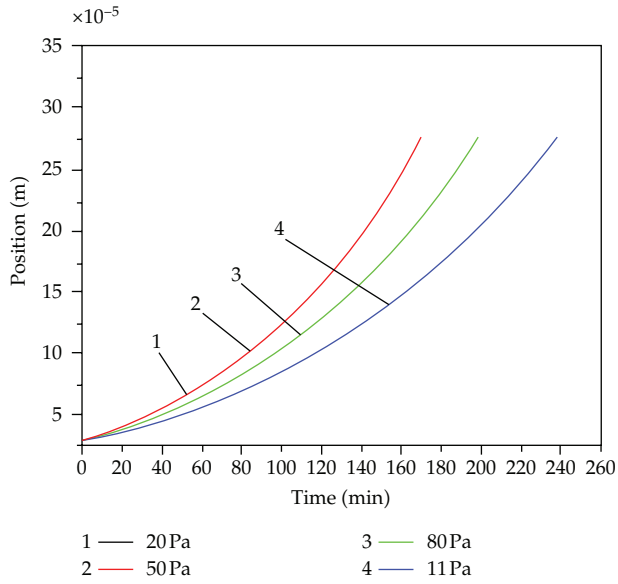

Figure 2: The calculated sublimation interface positions versus time at various chamber pressures.

of water vapor diffusion resistance at the sublimation interface and the rise of interface temperature [24–27], as shown in Figure 3. When the temperature of condenser's surface is constant, the interface temperature would be the main parameter to determine water vapor diffusion intensity. In previous studies, the interface temperature was assumed to be a constant value [28, 29], some experts believe that the assumption will decrease the simulation analysis precision, and they assume the sublimation interface temperature in the process of freeze-drying is gradually rising. They replace the constant interface temperature in the previous studies with the linear expression between the sublimation interface temperature and the location, thereby improving the mass transfer model in freeze-drying process. Figure 3 shows that when the sublimation interface of freeze-dried material moves 30 cm, its temperature just increases by 6°C, and corneal thickness is around 0.6 mm, so in this simulation, it is viable to assume the interface temperature is constant.

The temperature of sublimation interface, the temperature of condenser surface, and the pressure of freeze-drying chamber are correlated. If the temperature of sublimation interface is lower, the sublimation interface saturation pressure is lower accordingly, which requires the lower freeze-drying chamber pressure and lower condenser surface temperature. The relationship among them indicates that the saturation pressure of sublimation interface > the pressure of freeze-drying chamber > the saturation pressure of condenser surface. During the stages of a freeze-drying process, when the condenser surface temperature is −40°C, it affects little on shortening the time of freeze-drying. When the condenser surface temperature declines from −40°C to −100°C, the time of freeze-drying reduces just by 4%. The influence tends to be similar to the results of Millman's study on skim milk freeze-drying [30]. Too low temperature of the condenser surface does not greatly improve the differential pressure of water vapor diffusion, which is determined by the exponential function between the saturation pressure and temperature. Instead, if the sublimation interface temperature would be increased dramatically, which increases the differential pressure of water vapor

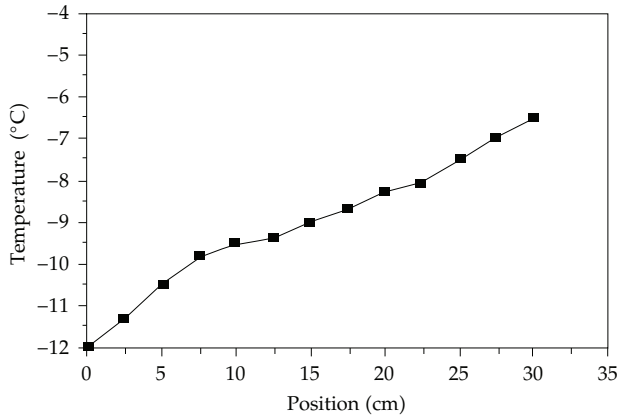

Figure 3: Relationship between temperature and position of sublimation interface.

diffusion (the saturated pressure is 260 Pa, when it is −10°C), the time of freezing can be reduced distinctly.

During the process of corneal freeze-drying, sublimation interface temperature cannot be in −30°C to −60°C, within which biological cells are at risk. If the temperature of the sublimation interface is below −60°C, it will not only reduce the temperature of the condenser surface, but also can make the time of freeze-drying much longer causing the increase of the damaged cornea chance. The experiment indicates that the corneal endothelial survival chance can achieve the standard value if the sublimation temperature is fixed around −10°C.

5.3. The Relationship between Differential Surface Temperature and the Time of Drying

Figure 4 shows the computational results of double-sided freeze-dried model of Figure 1. In Figure 4, the pressure in the freeze-drying chamber is 50 Pa, and the surface temperatures are −10°C, 0°C, and 10°C, respectively. Three curves are basic coincident, confirming that the variation of surface temperature is from −10°C to 10°C, it has little a influence on the corneal freeze-drying process.

5.4. Simulative Calculation Performed when the Pressure of Freeze-Drying Chamber Is 50 Pa and Corneal Surface Temperature Is 10°C

(1) The computational results illustrated in Figure 5 include two-sided freeze-dried model simulation and the change of sublimation interface with the freeze-drying process. As can be seen in the figure, in the initial stage of corneal freeze-drying, the position of sublimation interface moves quite smoothly. And at the end of drying, the slope of curve increases, which illustrates that the speed of the mobile sublimation interface increases. As the positive relationship between interface mobile rate and freeze-dried rate, the freeze-dried rate can be observed from the interface moving speed. Time of double-side freeze-drying was 170 mins.

(2) Figure 6 shows the results of the unit applying temperature and pressure load.

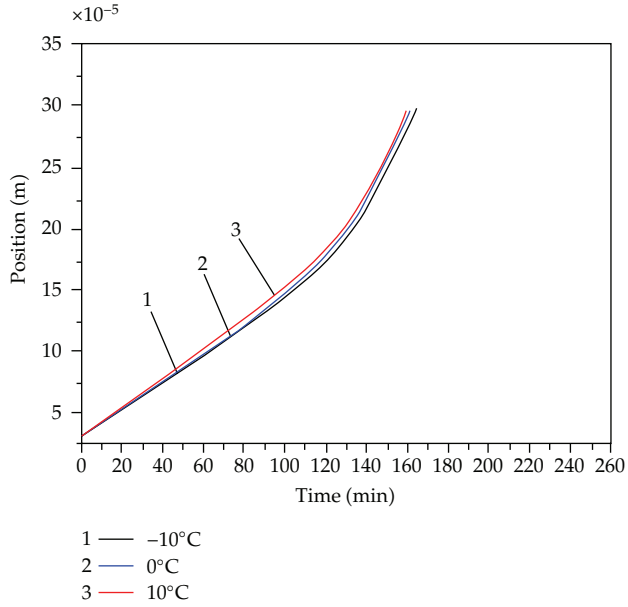

Figure 4: The calculated sublimation interface positions versus time at various surface temperatures.

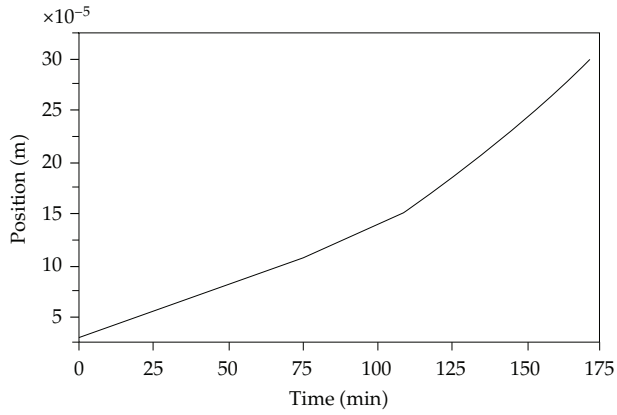

Figure 5: Relationship between position of sublimation interface and time.

6. Conclusions

(1) Mathematical model describing heat and mass transfer during vacuum freeze-drying of cornea is established through theory analysis of corneal freeze-drying. The analogy computation for the freeze-drying of cornea was made by using the finite-element computational software. When the pressure of the freeze-drying box is around 50 Pa and temperature is around −10°C, Time of double-side drying was 170 mins.

(2) In this paper, a moving-grid finite-element method is used to track the parameters node continuously to increase the experiment accuracy, also, the results are evident with clear physical significance.

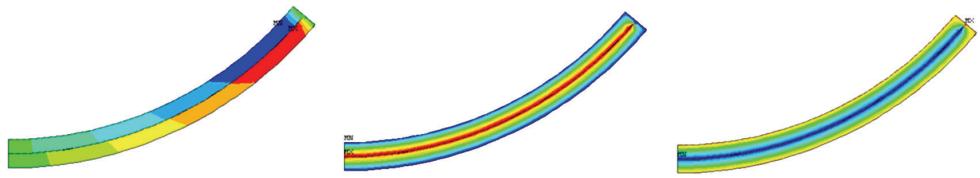

(a) (b) (c)

Figure 6: The flux pressure and temperature nephogram of cornea at the end.

Nomenclature

C_{sw}: Concentration of the water in the adsorption phase (or solid phase), the number of moles (or mass) per unit volume of frozen phrase (kg water/kg solid)
C_{pi}: Specific heat of the component i (kJ/kg·K)
C_{gi}: Concentration of the component I in gas phase, the number of moles (or mass) per space unit volume of frozen phase
N_i: The flow rate of the component i (kg/m^{2}s)
N_w: The flow rate of water vapor in the already dried layer (kg/m^{2}s)
N_{in}: The flow of permanent gas in the already dried layer (kg/m^{2}s)
N_{t}: Full flow in the already dried layer (kg/m^{2}s)
k: Coefficient of thermal conductivity (kW/m·K)
k_g: Coefficient of internal mass transfer with analytical function (s^{-1})
k_1: Diffusion rate constant of the main body $(C_2 D^0_{w,\text{in}} K_w / (C_2 D^0_{w,\text{in}} + K_{\text{mx}} P)$
k_2: Self-diffusion rate constant $(K_w K_{\text{in}} / (C_2 D^0_{w,\text{in}} + K_{\text{mx}} P) + (C_{01} / \mu_{\text{mx}})$
k_3: Diffusion rate constant of the main body $(C_2 D^0_{w,\text{in}} K_{\text{in}} / (C_2 D^0_{w,\text{in}} + K_{\text{mx}} P)$
k_4: Self-diffusion rate constant $(K_w K_{\text{in}} / (C_2 D^0_{w,\text{in}} + K_{\text{mx}} P) + (C_{01} / \mu_{\text{mx}})$
C_{01}: Constant only related to the structure of the porous media, which produce relative D'Arcy air permeability
C_1: Constant only related to the structure of the porous media, which can produce relative Knudsen air permeability
C_2: Constant only related to the structure of the porous media, which is the ratio of the main body diffusion rate to free gas diffusion rate, no dimension
K_{w}: Knudsen diffusion coefficient, $K_w = C_1 \sqrt{RT/M_w}$, where M_w is molecular weight of water
K_{in}: Knudsen diffusion coefficient, $K_{\text{in}} = C_1 \sqrt{RT/M_{\text{in}}}$, where M_{in} is molecular weight of permanent gas
K_{mx}: The average Knudsen diffusion coefficient of binary gas mixture, $(y_w K_{\text{in}} + y_{\text{in}} K_w)$
$D_{w,\text{in}}$: Diffusion coefficient of free gas in binary gas mixture with water vapor and permanent gas
R: Gas constant (kJ/mole·K)
M: Molecular weight (kg/kg mole)
P: Total pressure in the already dried layer (Pa)
P_w: Partial vapor pressure (Pa)
P^0_w: Initial partial vapor pressure (Pa)
P_{in}: Partial pressure of permanent gas (Pa)
P^0_{in}: Initial partial pressure of permanent gas (Pa)
q: Rate of heat flow (kW/m^2)

r: Radius (m)
t: Time (s)
T: Temperature (K)
T^0: Initial temperature (K)
T_∞: Outside temperature (K)
$T_{\text{int}\,f}$: Interface temperature (K)
v: Interface velocity (m/s)
x: Space coordinates through the thickness direction
y: Space coordinates through the warp direction
Y_i: The number of moles in the component i in gas phase
μ_{mx}: The viscosity of binary gas mixture with water vapor and permanent gas in porous already dried layer (kg/m·s)
ΔH_{v}: The vaporization heat of adsorbed water (kJ/kg)
ΔH_{s}: Latent heat of sublimation of ice (kJ/kg).

Greek Letters

ε: The volume of space in each unit volume of material;
ρ: Density, kg/m^3.

Subscript

i: Components
In: Permanent gas
w: Water
e: Effective value
I: Dried area
II: Freezing area
n: Quadrature component
x: X direction component
y: Y direction component.

References

[1] E.-N. Dragoi, S. Curteanu, and D. Fissore, "Freeze-drying modeling and monitoring using a new neuro-evolutive technique," *Chemical Engineering Science*, vol. 72, pp. 195–204, 2012.
[2] A. A. Barresi, R. Pisano, V. Rasetto, D. Fissore, and D. L. Marchisio, "Model-based monitoring and control of industrial freeze-drying processes: effect of batch nonuniformity," *Drying Technology*, vol. 28, no. 5, pp. 577–590, 2010.
[3] M. J. Pikal, S. Cardon, C. Bhugra et al., "The nonsteady state modeling of freeze drying: in-process product temperature and moisture content mapping and pharmaceutical product quality applications," *Pharmaceutical Development and Technology*, vol. 10, no. 1, pp. 17–32, 2005.
[4] R. Pisano, D. Fissore, S. A. Velardi, and A. A. Barresi, "In-line optimization and control of an industrial freeze-drying process for pharmaceuticals," *Journal of Pharmaceutical Sciences*, vol. 99, no. 11, pp. 4691–4709, 2010.
[5] N. Harnkarnsujarit, S. Charoenrein, and Y. H. Roos, "Microstructure formation of maltodextrin and sugar matrices in freeze-dried systems," *Carbohydrate Polymers*, vol. 88, no. 2, pp. 734–742, 2012.
[6] M. Terta, G. Blekas, and A. Paraskevopoulou, "Retention of selected aroma compounds by polysaccharide solutions: a thermodynamic and kinetic approach," *Food Hydrocolloids*, vol. 20, no. 6, pp. 863–871, 2006.

[7] A. Yongan, "High-efficiency low temperature drying equipment with heat hump," *Journal of Shenyang Architectural and Civil Engineering Institute*, vol. 12, no. 4, pp. 432–435, 1996.
[8] J. F. Nastaj and K. Witkiewicz, "Mathematical modeling of the primary and secondary vacuum freeze drying of random solids at microwave heating," *International Journal of Heat and Mass Transfer*, vol. 52, no. 21-22, pp. 4796–4806, 2009.
[9] J. F. Nastaj, K. Witkiewicz, and B. Wilczyńska, "Experimental and simulation studies of primary vacuum freeze-drying process of random solids at microwave heating," *International Communications in Heat and Mass Transfer*, vol. 35, no. 4, pp. 430–438, 2008.
[10] A. I. Liapis and R. J. Litchfield, "Optimal control of a freeze dryer-I: theoretical development and quasi steady state analysis," *Chemical Engineering Science*, vol. 34, no. 7, pp. 975–981, 1979.
[11] K. Georgiev, N. Kosturski, S. Margenov, and J. Starý, "On adaptive time stepping for large-scale parabolic problems: computer simulation of heat and mass transfer in vacuum freeze-drying," *Journal of Computational and Applied Mathematics*, vol. 226, no. 2, pp. 268–274, 2009.
[12] A. I. Liapis and R. J. Litchfield, "Numerical solution of moving boundary transport problems in finite media by orthogonal collocation," *Computers and Chemical Engineering*, vol. 3, no. 1–4, pp. 615–621, 1979.
[13] M. M. Tang, A. I. Liapis, and J. M. Marchello, "A multi-dimensional model describing the lyophilization of a pharmaceutical product in a vial," in *Proceedings of the 5th International Drying Symposium*, A. S. Mujumdar, Ed., pp. 57–64, Hemisphere Publishing Corporation, New York, NY, USA, 1986.
[14] M. J. Millman, A. I. Liapis, and J. M. Marchello, "An analysis of the lyophilization process using a sorption-sublimation model and various operation policies," *AIChE Journal*, vol. 31, no. 10, pp. 1594–1604, 1985.
[15] T. D. Tsvetkov and N. L. Vulchanov, "Toward the mathematical modeling of heat and mass transfer in vacuum freeze-drying. I. Thermodynamic analysis of heat- and mass-transfer processes in capillary porous materials undergoing freeze-drying," *Cryobiology*, vol. 18, no. 2, pp. 155–165, 1981.
[16] R. B. Evans, G. M. Watson, and E. A. Mason, "Gaseous diffusion in porous media. II. Effect of pressure gradients," *The Journal of Chemical Physics*, vol. 36, no. 7, pp. 1894–1902, 1962.
[17] A. Hottot, S. Vessot, and J. Andrieu, "Freeze drying of pharmaceuticals in vials: influence of freezing protocol and sample configuration on ice morphology and freeze-dried cake texture," *Chemical Engineering and Processing*, vol. 46, no. 7, pp. 666–674, 2007.
[18] C. Agnieszka and L. Andrzej, "Rehydration and sorption properties of osmotically pretreated freeze-dried strawberries," *Journal of Food Engineering*, vol. 97, no. 2, pp. 267–274, 2010.
[19] Z. Qinglian and L. Jianbo, "Contours and iso-surfaces drawing for the finite element method," *Journal of Shenyang Architectural and Civil Engineering University*, vol. 21, no. 3, pp. 220–224, 2005.
[20] J. Babić, M. J. Cantalejo, and C. Arroqui, "The effects of freeze-drying process parameters on Broiler chicken breast meat," *Food Science and Technology*, vol. 42, no. 8, pp. 1325–1334, 2009.
[21] K. Georgiev, N. Kosturski, S. Margenov, and J. Starý, "On adaptive time stepping for large-scale parabolic problems: computer simulation of heat and mass transfer in vacuum freeze-drying," *Journal of Computational and Applied Mathematics*, vol. 226, no. 2, pp. 268–274, 2009.
[22] T. Branger, C. Bobin, M.-G. Iroulart et al., "Comparative study of two drying techniques used in radioactive source preparation: freeze-drying and evaporation using hot dry nitrogen jets," *Applied Radiation and Isotopes*, vol. 66, no. 6-7, pp. 685–690, 2008.
[23] R. Thuwapanichayanan, S. Prachayawarakorn, J. Kunwisawa, and S. Soponronnarit, "Determination of effective moisture diffusivity and assessment of quality attributes of banana slices during drying," *Food Science and Technology*, vol. 44, no. 6, pp. 1502–1510, 2011.
[24] S. A. Velardi and A. A. Barresi, "Development of simplified models for the freeze-drying process and investigation of the optimal operating conditions," *Chemical Engineering Research and Design*, vol. 86, no. 1, pp. 9–22, 2008.
[25] J. Xiang, J. M. Hey, V. Liedtke, and D. Q. Wang, "Investigation of freeze-drying sublimation rates using a freeze-drying microbalance technique," *International Journal of Pharmaceutics*, vol. 279, no. 1-2, pp. 95–105, 2004.
[26] M. C. Olguín, V. O. Salvadori, R. H. Mascheroni, and D. A. Tarzia, "An analytical solution for the coupled heat and mass transfer during the freezing of high-water content materials," *International Journal of Heat and Mass Transfer*, vol. 51, no. 17-18, pp. 4379–4391, 2008.
[27] W. Y. Kuu, J. McShane, and J. Wong, "Determination of mass transfer coefficients during freeze drying using modeling and parameter estimation techniques," *International Journal of Pharmaceutics*, vol. 124, no. 2, pp. 241–252, 1995.

[28] M. Farid and R. Kizilel, "A new approach to the analysis of heat and mass transfer in drying and frying of food products," *Chemical Engineering and Processing*, vol. 48, no. 1, pp. 217–223, 2009.
[29] F. Rene, E. Wolff, and F. Rodolphe, "Vacuum freeze-drying of a liquid in a vial: determination of heat and mass-transfer coefficients and optimisation of operating pressure," *Chemical Engineering and Processing*, vol. 32, no. 4, pp. 245–251, 1993.
[30] M. J. Millman, A. I. Liapis, and J. M. Marchello, "Guidelines for the desirable operation of batch freeze dryers during the removed of free water," *Journal of Food Technology*, vol. 19, pp. 725–738, 1984.